Plane Stress Fracture Toughness Evaluation of Removable Radial Shield Assembly Materials

D.E. McCabe, W.A. Logsdon
Westinghouse Electric Corporation R+D Center, 1310 Beulah Road, Pittsburgh, Pennsylvania 15235, U.S.A.

SUMMARY

The principal objective of this program was to determine the suitability of small surveillance specimens, such as precracked Charpys and small compact specimens to detect and accurately represent toughness changes in 316 stainless steel from irradiation damage. The materials were 316 stainless cold rolled 20% as baseline and cold rolled 50% to simulate the irradiation damaged condition. Specimens were: standard compacts 3.2 mm (0.125 inch) thick but of 1/2T, 1T and 4T plan view sizes. J_R-Curves were developed and these were compared to results from subsize Charpys, both precracked and machine notched, and single edge tension, SE(T) specimens. All were constant thickness at (0.125-inch) 3.2 mm. Loading was both static and dynamic. Whenever possible, toughness evaluation was by J and the J_R-Curve behaviors.

The J_R-Curve behavior was found to be specimen size and geometry independent. Increased cold reduction from 20% to 50% increased strength and reduced toughness. These effects were observed in all specimen types and sizes from Charpy size to SE(T) size. Dynamic strain rates increased strength and lowered J_R-Curve toughness. Trends established by J_R-Curve were always evident in the Charpy results.

1. Introduction

The design of the Clinch River Breeder Reactor (CRBR) calls for extensive use of 316 stainless steel sheet, cold rolled to obtain a desired strength level. A material property of primary concern is the fracture toughness, both before and after irradiation exposure. The material is cold rolled approximately 20% to 1.5 mm (0.060-inch) thickness and is formed into hexagonal shaped ducts which hold shield rods. The component of principal interest here is the removable radial shield assemblies (RRSA) shown in greatest detail in Figure 1. The function of these is to shield the permanent reactor containment structure from neutron irradiation damage and these removable shield rod assemblies can be replaced when their damage level becomes critical as assessed by surveillance specimens. Four of the many radial shield assemblies in the CRBR are to contain surveillance specimens, and these are exposed in 25 mm (1-inch) diameter tubes inserted as a subassembly. Specimens are presently slated to be tensiles and Charpys, and fracture mechanics type specimens could be included, provided they can be designed to fit within the 25 mm (1-inch) available space of the container tube.

The specific concerns that the present project was intended to address are:

i) determine if the relatively small Charpy specimen is adequately sensitive to evaluate changes in toughness due to irradiation damage, and

ii) evaluate the feasibility of small fracture mechanics specimens of a size that can be fit into the surveillance tubes. Compare small versus large specimen J_R-Curves.

2. Experimental Approach

Commercially available 316 stainless steel sheet was obtained in 0.32 m (12.5 inch) wide pieces which were subsequently cold rolled 20% or 50% down to about 3.8 mm (0.15 inch) thickness. Chemistries and the as cold reduced mechanical properties are reported in Table I. Finished thickness for all test specimens was 3.2 mm (0.125 inch). The 20% reduction (Heat 70670) was to simulate the properties of the casing or duct materials prior to radiation exposure and the 50% reduction (Heat 26452) was intended to simulate the damaged condition of post irradiation exposure. The cold reduction was performed in a laboratory cold mill with no tension load on the strip, and some difficulties developed with shape control. The final shape of the strips was too wavy to obtain good center cracked tension panels to satisfy an original experiment objective. A compromise decision was made to make single edge notched [SE(T)] specimens instead. The loading of SE(T) specimens with short initial cracks ($a_o/W \leq 0.3$) approaches that of equal parts tension and bend components, and as such, the value of this test for comparison purposes would be somewhat similar to data obtained from the much larger center cracked tension specimens. An appropriate analysis to calculate J on the SE(T) geometry has just recently been developed by Ernst [1] and the equation along with the needed calibration coefficients is shown in Figure 2. The revised scope of specimens tested is illustrated in Figure 3. The specimens are shown here to a proportional scale.

Another concern was the effect of strain rate on the fracture toughness of the 316 stainless materials. In the present project, these tests were performed at an exaggerated rate in comparison to that of concern for in service application; i.e. under seismic loading.

3. Testing Procedure

Compact specimens were tested under displacement controlled loading. Crack growth was measured using an unloading compliance method, [1] and whenever possible, this was supplemented with visual measurement of crack growth on the specimen surfaces. The load-line displacement was measured with a clip gage and the attachment points on the specimen were razor blades, spot welded on at the load-line position. For unloading compliance measurement of crack growth, an enlarged scale load-displacement test record was used to improve the sensitivity of slope measurement. A typical data set obtained from a test on a 1/2T specimen is shown in Table II. Note the column containing the crosshead LVDT output or ram position voltage. This information was used in conjunction with clip gage output to establish ram stop positions in dynamic loading rate tests. At dynamic rates, clip gages tend to be unstable and it was necessary to infer load line displacement from the more stable ram position voltage. The technique applied to dynamic J_R-Curve development was a multiple specimen method where each specimen gives only one J_R-Curve data point. Three specimens were available per dynamic test condition. Although the results look satisfactory here, the numbers of data points will not satisfy ASTM requirements. Nevertheless, the trend in behavior with strain rate will be quite clear. Load versus cross-head voltage was recorded on an image retaining oscilloscope and load line displacement was inferred using Table II type test information from psuedo static tests.

For Charpy testing, subsize specimens [3] were used where the specimen thickness was 3.2 mm (0.125 inch). Width was the standard 10 mm (0.394-inch). Some specimens had the standard 2 mm (0.08-inch) deep V-notch while others were precracked in fatigue to a relative crack depth (a_o/W) of about 0.5.

For dynamic Charpy tests, an instrumented impact tup was used and it was possible to determine energy to maximum load as well as the total energy to fracture. With slow loaded Charpy tests, a three point bend loading jig was used in a servo-hydraulic controlled test machine. In this equipment, center point displacements greater than about 6.3 mm (0.25-inch) tended to develop test jig interferences (jamming of the specimen) and, for the 20% cold rolled material, the tests could not be carried through to complete separation of the specimens.

Single edge notched SE(T) specimens were tested in flat bottom hole clevises which are ordinarily used to test 2T size compact specimens. The specimens were fully supported in the grip area against buckling about the loading pins. The test procedure was identical to that used on compact specimens with a clip gage mounted on knife edges across the crack mouth. Crack growth was monitored visually in this case because the unloading compliance equations had not been developed for this particular specimen geometry. Visual measurement is not completely accurate because plastic zone development tended to obscure the visual identification of the physical crack tip, and as such, the measurements were correct to about the nearest 1.3 mm (.05 inch). Hence the resulting J_R-Curves from SE(T) were a little crude in comparison to those developed in compact specimens with unloading compliance.

4. Fracture Toughness Representation

4.1 Compact Specimens

The toughness characteristics of 316 stainless steel are such that brittle instability is never expected to develop. A running crack condition can occur only by plastic collapse after stable crack growth to a condition of maximum load. Prior to this, running crack conditions are resisted by the R-Curve toughness development in the material. Therefore, the toughness comparison between various metallurgical conditions of 316 stainless should be made comparing J_R-Curves where the toughness is expressed in J_R units, energy/crack area.

In past years, the use of J has been questioned in J_R-Curve work because of an incompatability between the original deformation theory assumption and slow-stable crack growth. The following expression has been recently developed by Ernst et al. [4] to correct deformation theory J for growth in compact specimens:

$$J_{i+1} = \left[J_i + \left(\frac{\eta}{b}\right)_i \frac{A_{i,\,i+1}}{b}\right] \left[1 - \left(\frac{\gamma}{b}\right)_i \left(a_{i+1} - a_i\right)\right] \qquad (1)$$

and $\eta = 2 + .522\ b/W$

$\gamma = 1 + .76\ b/W$

$A_{i,i+1}$ = incremental work applied between steps i and i+1.

4.2 Single Edge Notched SE(T)

Ernst has also recently developed an expression to calculate J for the SE(T) geometry [1], Figure 2.

$$J = G + \left(\frac{\gamma}{b}\right) \int_o^{\delta^*} P\, d\delta_* - \left(\frac{\beta}{b}\right) \int_o^{P} \delta_*\, dP \qquad * \text{ plastic component} \qquad (2)$$

However, Equation (2), unlike Equation (1), is for a non-growing crack situation, and the corresponding form to Equation (1) is not yet available. Therefore, when we chose to compare SE(T) to compact specimen J_R curves, the compact data was recalculated without the growth correction of Equation (1).

4.3 Instrumented Cnarpy

In Charpy tests, crack growth could not be measured and J_R-Curves were not possible for comparisons. However, J_R can be crudely estimated at various deformation levels on the fatigue precracked specimens using:

$$J = 2\left(\frac{W}{A}\right) \qquad (3)$$

W/A - work divided by the initial remaining ligament area.

Crack growth in the Charpy specimens in all probability initiates just beyond maximum load in all cases, and could be used as a suggestion (right or wrong) that J_R at P_{max} roughly estimates J_{Ic}.

5. Test Results

5.1 Geometry Effects on J_R-Curve

The J_R-Curves generated from duplicate 1/2T compact specimens are shown in Figure 4. They indicate that toughness decreases due to an increase in cold reduction. J at crack initiation (intersection with the blunting line) is approximately 140 KJ/m^2(800 in-lbs/in^2) for 20% cold reduced material and about 53 KJ/m^2(300 in-lbs/in^2) with 50% cold reduction. Crack growth resistance develops more readily in the 20% cold reduced material.

The larger 1T and 4T compact specimen data are plotted against the 1/2T J_R-Curves in Figure 5. There are fewer data points and more scatter in the 4T tests because it was difficult to maintain the precision and frequency of measurement of crack size with the larger specimens. Nevertheless, it appears that the J_R-Curve is independent of specimen size, which fortunately supports a fundamental J_R-Curve principle. J_R-Curves developed from SE(T) specimens are shown in Figures 6 and 7 and these are compared to data from 1/2T compact specimens. Again, it should be emphasized that J was calculated without correction for crack growth in both cases; viz, the 1/2T compact data was reworked. The J_R-Curve data for the two specimen types tended to be geometry independent until the onset of limit load for the SE(T) specimens. The SE(T) specimen with $a_o/W = 0.3$ has a bend to tension loading ratio of 1.3/1 as opposed to 12/1 for compact specimens. This evidence suggests that J_R-Curve behavior for these materials tends to be independent of loading mode and that the general J_R-Curve principle of geometry independence can be utilized in the present application.

5.2 Loading Rate

Compact specimens were dynamically loaded at $J = .7 \times 10^4$ KJ/m^2/sec ($K = 2.2 \times 10^4$ MPa$\sqrt{m}$/sec rate, stopping the loading of specimens in mid-test. Three specimens gave three levels on the dynamic J_R-Curve with final crack size determined by heat tint. Figure 8 compares slow and dynamic load-displacement records for 1/2T size compact specimens of the material that was 50% cold rolled. Strength is slightly increased and the crack growth resistance is also decreased. The J_R-Curve comparison is made in Figure 9.

5.3 Charpy Results

Charpy tests [5] were made on the two materials with the test variables of strain rate (Impact vs Slow Load) and notch sharpness (Standard Charpy V vs Precracked). Since the testing was performed with instrumented tup equipment, values of sharp crack fracture toughness corresponding to maximum load could be roughly estimated if the precracked Charpy specimens are considered. The toughness at maximum load could possibly relate to J_{Ic} and the data in Table III lists these results. These data demonstrate the same trends that the compact fracture mechanics specimens had shown, namely that:

i) 20% cold reduced material has higher toughness than the 50% cold reduced material.

ii) Touhness estimates of J_{Ic} from Precracked Charpys are high but they do in fact rank the toughness of the two materials appropriately.

iii) Increased strain rate increases the material strength. The total toughness is reduced due to some loss in crack growth resistance; similar to the J_R-Curve indicated toughness drops.

Again, the total energy to fracture comparison on 20% cold rolled material (Heat 70670) was unobtainable because of the loading jig which could not develop the total displacement needed to completely separate the specimen.

6. Conclusions

The J_R-Curve behavior of both 20 and 50% cold rolled 316 stainless steel was found to be independent of specimen geometry effects. The J_R-Curve of 50% cold rolled material had a lower crack initiation J_{Ic} and lower J_R-Curve slope.

The small Charpy specimens, either precracked or with a standard machined notch, proved to have the same toughness trends as the standard fracture mechanics specimens. Estimating J_{Ic} at maximum load from Precracked Charpys, however, gave values that were high by a factor of about 3.

Dynamic loading with K in the order of 2.2×10^4 MPa$\sqrt{m}$/sec showed increased strength and reduced fracture toughness compared to static loading.

7. Acknowledgement

The authors would like to acknowledge the efforts of Mr. W. H. Pryle, who organized the specimen preparation part of this program. In the Mechanics of Materials Group, special thanks must go to Messrs E. J. Helm and L. W. Burtner, who performed most of the tests and in the Materials Testing and Evaluation Lab., Mr. R. B. Stouffer who tested the Charpy specimens. This work was sponsored by the Advanced Reactor Division of Westinghouse under DOE contracted research. The authors would like to acknowledge the help received from Messrs A. Kasberg and V. Sazawal of ARD.

8. References

(1) Ernst, H. A., "Unified Solution for J Ranging Continuously from Pure Bend to Pure Tension," Presented at 14th NSFM, July 1, 1981, Los Angeles, CA, to be published, ASTM.

(2) Clarke, G. A., Andrews, W. R., Davis, R. C., and Schmidt, D. W., "Single Specimen Tests for J_{Ic} Determination," Mechanics of Crack Growth, ASTM STP 560, 1976, pp. 27-42.

(3) ASTM Standard Method E23, Book of Standards, Part 10, 1981.

(4) Ernst, H. A., Paris, P. C., and Landes, J. D., "Estimations on J-Integral and Tearing Modulus T, from a Single Specimen Test Record," Proceedings of 13th NSFM, Philadelphia, PA, 1980.

(5) Bush, A. J., Stouffer, R. G., "Instrumented Charpy Fracture Tests on 70670 and 26452 Material," Westinghouse Report 80-71343, Oct. 29, 1980.

(6) Tada, H., Paris, P. C., and Gamble, R. M., "A Stability Analysis of Circumferential Cracks for Reactor Pipe Systems ASTM STP 700, 12th NSFM, 1980, pp. 296-313.

Table I

Material-316 Stainless, ASTM A240

Heat Number	Source	Processing*	Initial Dimensions(inches)
70670	Eastern	20% cold reduction	12.5 x 40 x 0.1875
26452	Jessop	50% cold reduction	12.5 x 25 x 0.250

*The laboratory cold rolling mill at USS Research Laboratories was used. No coil tension or flattening applied.

Chemistry

	C	Mn	P	S	Si	Cr	Ni	Cu	Mo	N
70670	.040	1.66	.01	.006	.61	17.63	11.17	.14	2.11	.038
26453	.067	1.70	.03	.012	.51	16.30	11.20	.35	2.15	.043

Mechanical Properties

	Yield Strength ksi	(MPa)	Tensile Strength ksi	(MPa)	%El	%Ra	HRB
70670	109.3	(754)	121.7	(839)	229	55.3	63.5
26452	144.5	(996)	165.5	(1141)	95	38.3	67.5

Table II

Typical Data on 1/2T CT Specimens
Thickness 3.2mm(0.125-inches), $a_o/W = 0.6$

Code 70670-1
B = 3.2mm(0.125 in.)
a_o = 15mm(0.6 in.)

Static Loading

Event	P(N)	v_{LL}(mm)	Ram Volts	Δa_p(mm)*	kJ/m^2(in-lbs/in^2)	
1	2.22	.350	.505	0	37	(152)
2	2.94	.746	.990	.051	96	(549)
3	3.11	1.153	1.37	.178	178	(1015)
4	3.14	1.524	1.68	.254	256	(1461)
5	3.09	1.905	1.97	.330	335	(1916)
6	2.91	2.273	2.24	.610	398	(2275)
7	2.76	2.667	2.53	.864	462	(2643)
8	2.54	3.063	2.81	1.118	521	(2980)
9	2.38	3.432	3.08	1.626	548	(3132)
10	2.22	3.810	3.35	1.981	586	(3347)

*10 volts full scale for 0.50-inch ram displacement

Table III

Charpy Results

I. Precracked Charpy

Mat.	P_{max},N(lbs) Static	Impact	Total Energy, W/A KJ/m^1(in-lbs/in^2) Static	Impact	Estimate* J_{Ic},KJ/m^2(in-lbs/in^2) Static	Impact
70670(20%CR)	2670(600)	2945(662)	≠	1085(6200)	380(2170)	468(2675)
26452(50%CR)	2850(640)	3115(700)	434(2480)	350(2000)	175(1000)	202(1155)

II. Standard Machined Notch

Mat.	P_{max}, N(lbs) Static	Impact	Total Energy, W/A Static	Impact
70670(20%CR)	6450(1450)	7965(1790)	≠	1485(8540)
26452(50%CR)	7410(1665)	7920(1780)	756(4320)	626(3580)

* J_{Ic} = 2(W/A at P_{max})

≠ Specimen not completely separated
Last W/A precracked = 710 KJ/m^2
Last W/A Std notch = 7280 KJ/m^2

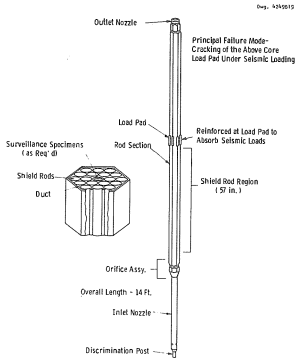

Fig. 1—Removable radial shield subassembly

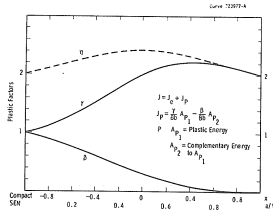

Fig. 2—Plastic factor η, γ, and β vs generalized coordinate x and single edge notch a/W

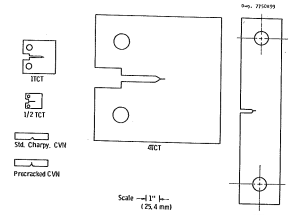

Fig. 3—Comparison of the various specimen geometries considered in this program

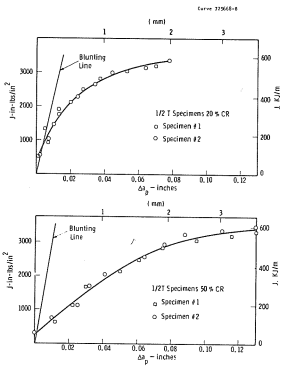

Fig. 4—J_R-curves from 1/2T specimens of 316 stainless steel. Top 20 % cold rolled, bottom 50 % cold rolled.

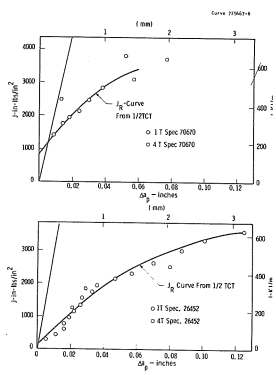

Fig. 5—J_R curves from1/2T specimens and data points from 1T and 4T compact specimens

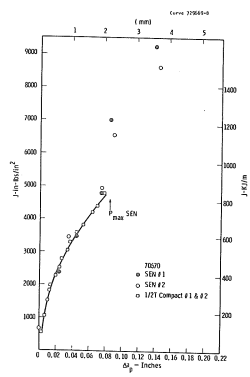

Fig. 6—J_R-curve for 1/2T compact and SEN data. 316 stainless, 20 percent cold rolled.

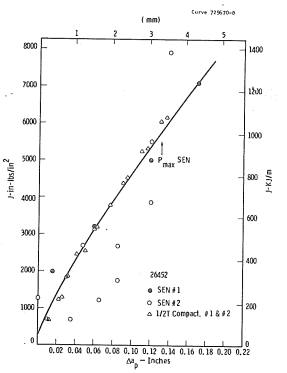

Fig. 7—J_R-curve for 1/2T compact and SEN data. 316 stainless, 50 percent cold rolled.

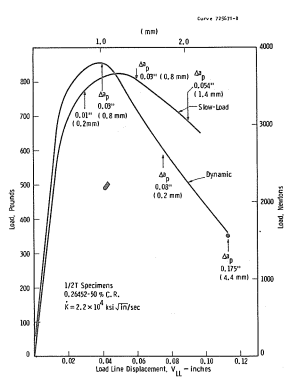

Fig. 8—Static and dynamic load versus displacement test records.

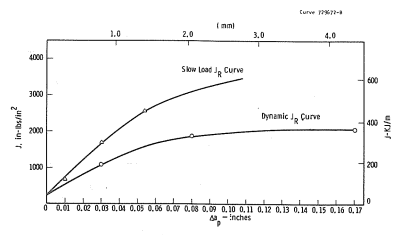

Fig. 9—J_R curves for 50 % cold rolled material (Ht 26452) static versus dynamic loading.